†Work supported by the U. S. Atomic Energy Commission.

*Present address: State University of New York College at Fredonia, Fredonia, New York.

[1]H. Hübel, R. A. Naumann, M. L. Andersen, J. S. Larsen, O. B. Nielsen, and N. O. Roy Poulsen, Phys. Rev. C **1**, 1845 (1970).

[2]R. S. Hager and E. C. Seltzer, Nucl. Data A4, 1 (1968).

[3]S. G. Nilsson, Kgl. Danske Videnskab. Selskab, Mat.-Fys. Medd. 29, No. 16 (1955).

[4]M. Jørgensen, O. B. Nielsen, and G. Sidenius, Phys. Letters 1, 321 (1962); E. Bodenstedt, J. Radeloff, N. Buttler, P. Meyer, L. Schänzler, M. Forker, H. F. Wagner, K. Krien, and K. G. Plingen, Z. Physik 190, 60 (1966).

Four-Parameter Measurements of Isomeric Transitions in ^{252}Cf Fission Fragments*

Walter John, Frank W. Guy,† and J. J. Wesolowski

Lawrence Radiation Laboratory, University of California, Livermore, California 94550
(Received 5 June 1970)

The γ rays emitted from 3 to 2000 nsec after spontaneous fission of ^{252}Cf have been studied in detail. Both fission fragments were stopped on Si detectors; a Ge detector was used to detect γ rays from the fragments on one Si detector. A time-to-amplitude converter was started on the fission-fragment signal and stopped on the γ-ray signal. For each event the two fission-fragment kinetic energies, the γ-ray energy, and the time delay were recorded. The data were then analyzed to obtain the energy, half-life, and intensity of each γ ray as well as the mass of the emitting fission fragment. Some 144 γ rays were so analyzed, corresponding to more than 80 isomeric states.

γ rays were observed from practically all masses. However, the intensity was concentrated in the mass regions near 96, 108, 134, and 146. The energy spectrum consisted of a group of γ rays below 500 keV and a group near 1300 keV. The high-energy group associated with masses 134 and 136 dominates the energy intensity after 50 nsec. A strong cascade from a 162-nsec isomeric state is assigned to $^{134}_{52}$Te$_{82}$, and a 3000-nsec isomeric state to $^{136}_{54}$Xe$_{82}$. Rotational cascades were not observed, in contradiction with earlier low-resolution work. The observed energies and half-lives can be accounted for by $E1$, $M1$, or $E2$ transitions, either allowed or K forbidden by a few units. The interpretation of these results is that the initially high spins of the fragments have less effect on the delayed γ rays than was previously thought.

Fragment kinetic energy distributions were obtained for fissions leading to the emission of a particular γ ray. The γ ray serves to restrict the events to those having a definite final isotope for one fragment. The average kinetic energy of such events is found to be slightly greater than the average for all fissions yielding the same mass.

I. INTRODUCTION

Fission fragments deexcite by first emitting neutrons and then γ rays. The bulk of the γ radiation has a half-life of the order of 10^{-11} sec.[1,2] A delayed[3] component in the time region of 50 nsec to 10 μsec after thermal-neutron-induced fission of ^{235}U was first observed by Maienschein *et al.*[4] Further measurements were made by Johansson[5] on γ rays from spontaneous fission of ^{252}Cf in the time range 10–300 nsec and by Popeko *et al.*[6] on ^{235}U fission from 10–70 nsec. Walton, Sund, and their collaborators[7–9] observed isomeric[10] γ rays with half-lives from 2 to 600 μsec following fission.

Johansson[5] measured the mass distribution of the γ rays for the time interval 30 to 70 nsec after fission and found it to be strongly peaked at certain masses. In these mass regions the fraction of the γ rays which were delayed was found to be surprisingly high. This high probability of populating isomeric states was attributed to the comparatively high initial spins of the fission fragments. These are neutron-rich nuclei which are normally inaccessible for study. The peaking of the intensity of delayed γ rays at certain masses is dependent on the nuclear structure of the fragments. Thus there are interesting features of the delayed γ rays deserving of further investigation.

In the present work the use of semiconductor detectors made it possible to measure the energies, intensities, and half-lives of individual γ rays and to determine the masses of the emitting fission fragments. The experiment covered the time range from 3 to 2000 nsec after fission.

II. EXPERIMENTAL PROCEDURE

A. Experimental Arrangement

The geometry of the experiment is shown in Fig. 1. A thin source of ^{252}Cf was positioned between two Si diodes which detected the oppositely directed fragments from a fission event. A Ge(Li) crystal located near one of the Si detectors detected γ rays emitted by fragments stopped on that Si detector. The Si detector was inclined 23° from the normal to present a clear path for the γ rays. A collimator of tungsten alloy served to shield the Ge detector from the ^{252}Cf source. This defined the fragment emitting the γ ray and eliminated most of the prompt γ rays. The inside edges of the collimator were serrated to minimize scattering of fission fragments. The ^{252}Cf source was prepared by self-transfer onto 90-μg/cm^2 Ni foil and had a strength of 46 μCi.

For each event four parameters were measured: the kinetic energies of the two fission fragments, the energy of the γ ray, and the time delay between the arrival of the fragment on the inclined detector and the detection of the γ ray.

B. Detectors

Phosphorous-diffused Si p-n junctions were used for fission-fragment detection. The diodes were fabricated from 2900-Ω-cm Si and were 3 cm^2 in area. Aluminum collimators with rounded edges were used to exclude the fringe area of the detectors. The detectors were cooled to −40°C in order to keep the leakage current low as radiation damage accumulated. It also appears that a higher
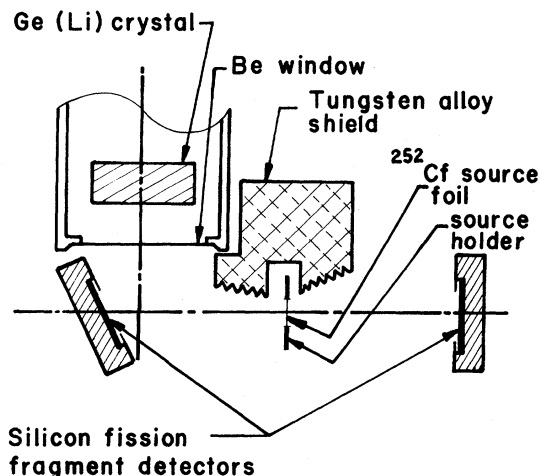
FIG. 1. Schematic drawing of the experimental apparatus, top view.

radiation dose can be tolerated at lower temperatures. The resolution for fission fragments (peak-to-valley) was 2.85 to 2.90 initially and 2.75 to 2.80 after data taking. Molecular-sieve pumps were used to maintain the vacuum in the experimental chamber.

The Ge(Li) crystal was a 9-cm^3 planar detector. A 10-mil Be window separated the Ge crystal from the vacuum chamber. Some tailing of the γ-ray peaks developed during the data runs owing to radiation damage from the fast fission neutrons. The resolution was affected somewhat and was 2-keV full width at half maximum (FWHM) for ^{57}Co (122 keV) and 4 keV for ^{60}Co (1.33 MeV).

C. Electronics and Calibration

A diagram of the electronics is shown in Fig. 2. A fast coincidence (30 nsec) was required between the two fission pulses. The time-to-amplitude converter (TAC) was started on the fission-fragment signal and stopped on the γ-ray signal from the Ge detector. A slow coincidence was then required between the TAC output and the fast fission coincidence output. Pileup inspector circuits examined the fast fission pulses to exclude any events having more than one pulse within 2 μsec. This prevented pileups between the numerous α particles and the fission fragments. The linear signals were digitized by a four-parameter pulse-height analyzer having 4096 channels per parameter and recorded on magnetic tape for subsequent computer analysis.

The TAC was adjusted to cover fission-γ-ray delay times from −150 to 2050 nsec. The negative-time data were used to evaluate the accidental-coincidence rate which was 17% of the data rate, averaged over the entire 2-μsec range. A time spectrum of all the events is shown in Fig. 3. It can be seen that the proportion of accidentals depends on the delay time.

Considerable energy-dependent walk was present in the time signal from the Ge detector. This was taken out in the computer analysis. The corrected timing resolution for all γ rays was 3 nsec FWHM. At 1 MeV it was 2 nsec FWHM, increasing to approximately 10 nsec at 100 keV. At long times an oscillation in the counts versus time display of Fig. 3 is evident, with a period of about 200 nsec. This effect was noted in the preliminary setup work and was apparently eliminated by minor modifications to the electronics. The effects became visible again after the data were computer-corrected for energy walk.

Stabilization of the electronics was accomplished with a precision pulser. For the γ-ray linear signal both the gain and zero level were stabilized;
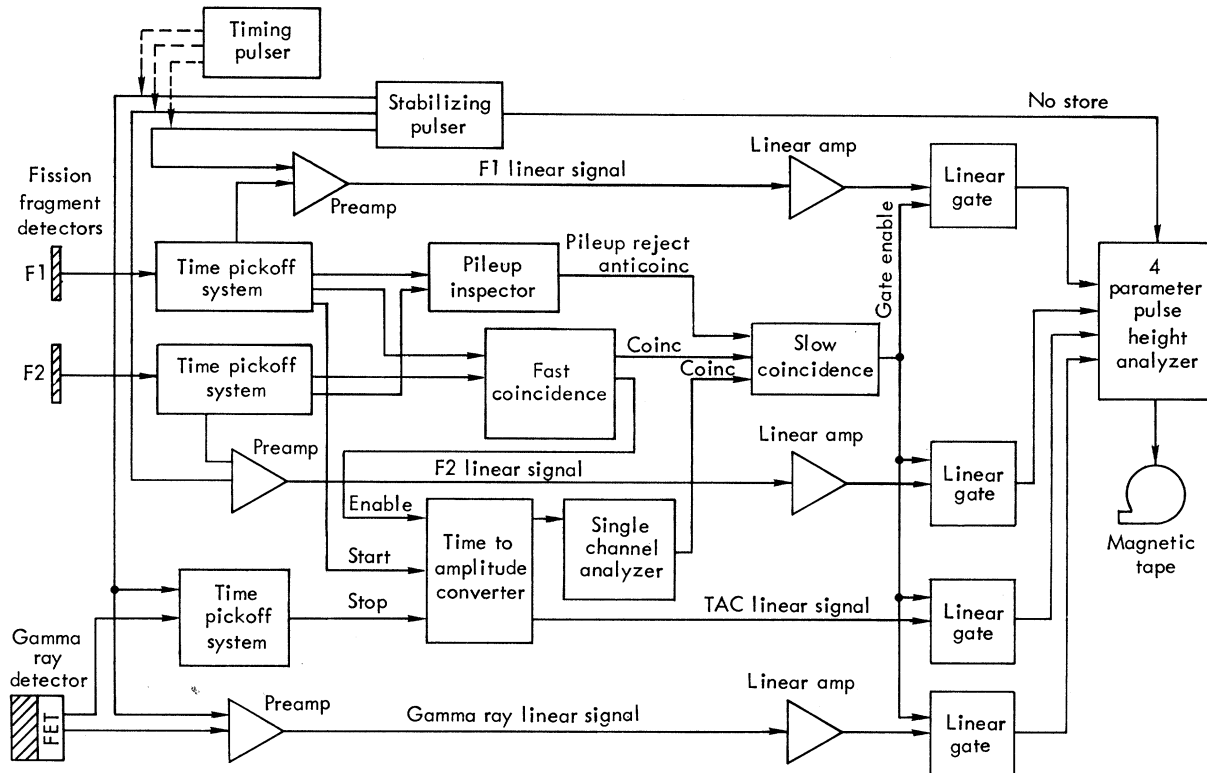
FIG. 2. Block diagram of the electronics.

for fission-fragment linear signals only the gains were stabilized. During the data runs the pulse heights of the fission-fragment spectum decreased gradually as radiation damage to the detectors accumulated. Periodic calibration runs were made with the logic altered to require only fission-fragment–fission-fragment coincidences.

The discriminator on the γ-ray time pickoff was set at 80 keV, and the analyzer spanned the γ-ray energy region up to 3 MeV. Some difficulty from multiple pulsing was encountered for lower dis-
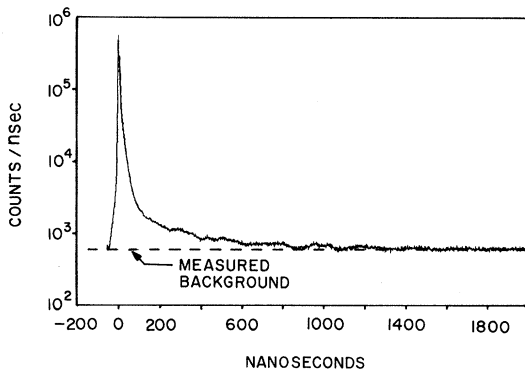
FIG. 3. Time distribution of all four-parameter events.

criminator settings, but one run was made down to 50 keV. The linearity of the γ-ray energy scale was measured with standard sources. Small shifts (<0.2 keV) in the energy scale from run to run were corrected by matching certain prominent peaks in the delayed γ-ray spectrum. The absolute energy scale was determined by two lines present in all the data, namely, the 511.00-keV annihilation line and a background peak from the 1293.64-keV γ ray of ^{41}Ar. The latter was present in the environment because of the proximity of the Livermore reactor. In addition, at 197.1 keV a line was observed which was associated with a broad range of masses and had a half-life of ~60 nsec. This was identified with an isomeric transition in ^{19}F, produced by inelastic scattering of the fission neutrons from ^{19}F in Teflon located near the Ge crystal. The observed energy is in excellent agreement with the value 197.146 ± 0.012 keV recently determined by White[11] in this laboratory. It should be noted that since the fission fragments were stopped on the Si detector, there was no shift of γ-ray energy and no line broadening from the Doppler effect except in the cases of a few very short-lived γ rays. In previous fission–γ-ray experiments using NaI detectors considerable difficulty was encountered from the neutron background.[2]
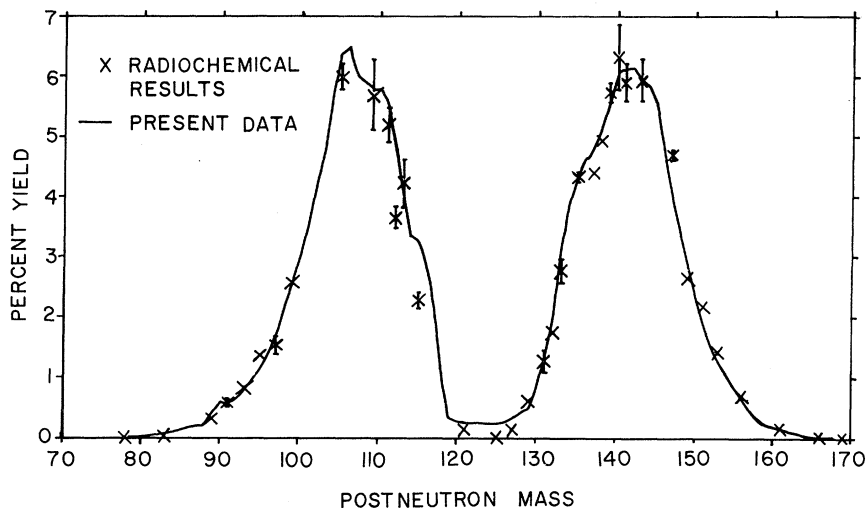
FIG. 4. Comparison of the fission-fragment postneutron mass distribution derived from the two-parameter (fragment-fragment) data in the present experiment (line) with the results of radiochemistry (crosses).

Ge detectors are less sensitive to neutrons; however, the spectra obtained in the present experiment exhibit some neutron-produced lines, particularly the prominent asymmetric 690-keV line[12] from ^{72}Ge. These neutron-produced lines could be easily distinguished from the fission-fragment γ rays, since they were not associated with a particular fission-fragment mass.

The count rate during the four-parameter data runs was 380 min^{-1}. Data were taken in 11 runs comprising a total of 7×10^6 events. Each of the 11 runs was preceded and followed by a two-parameter fission-fragment–fission-fragment calibration run.

III. ANALYSIS AND RESULTS

A. Mass Calculation

For each event the fission-fragment mass was calculated from the measured pulse heights of the two fission-fragment signals following a procedure similar to that devised by Watson.[13] A correction for neutron emission was made using the data of Bowman et al.[14] For this purpose the neutron data were fitted by the function

$$\nu(M^*, E_T^*) = A(M^*)\exp[B(M^*)(E_T^* - 150)] ,$$

where ν is the number of neutrons emitted by the fragment with pre-neutron-emission mass M^*, E_T^* is the total pre-neutron-emission fragment kinetic energy, and A, B are constants.

Pulse heights were converted to energies through the equations given by Schmitt, Kiker, and Williams,[15] which correct for the mass-dependent "pulse-height defect." Constants for the equations were obtained from fits to the two-parameter fission-fragment calibration runs. The mass calculation, including the correction for neutron emis-
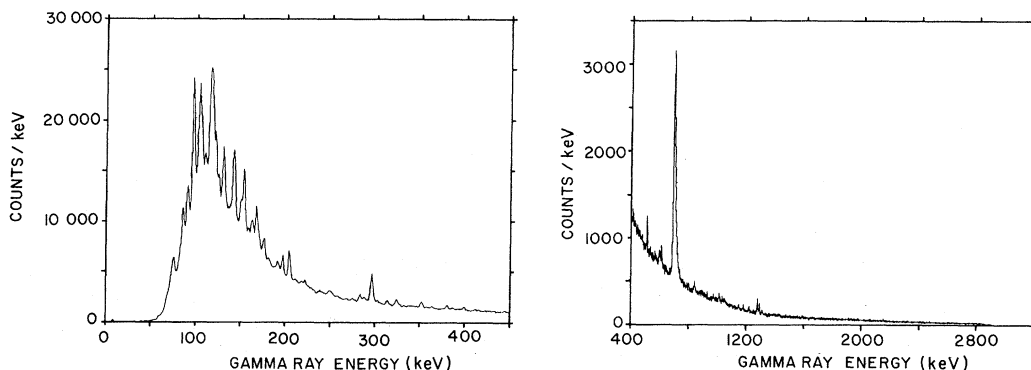
FIG. 5. The total fission γ-ray spectrum for times from 10 to 2000 nsec after fission. The large peak at 690 keV is produced by inelastic scattering on neutrons from ^{70}Ge in the detector.
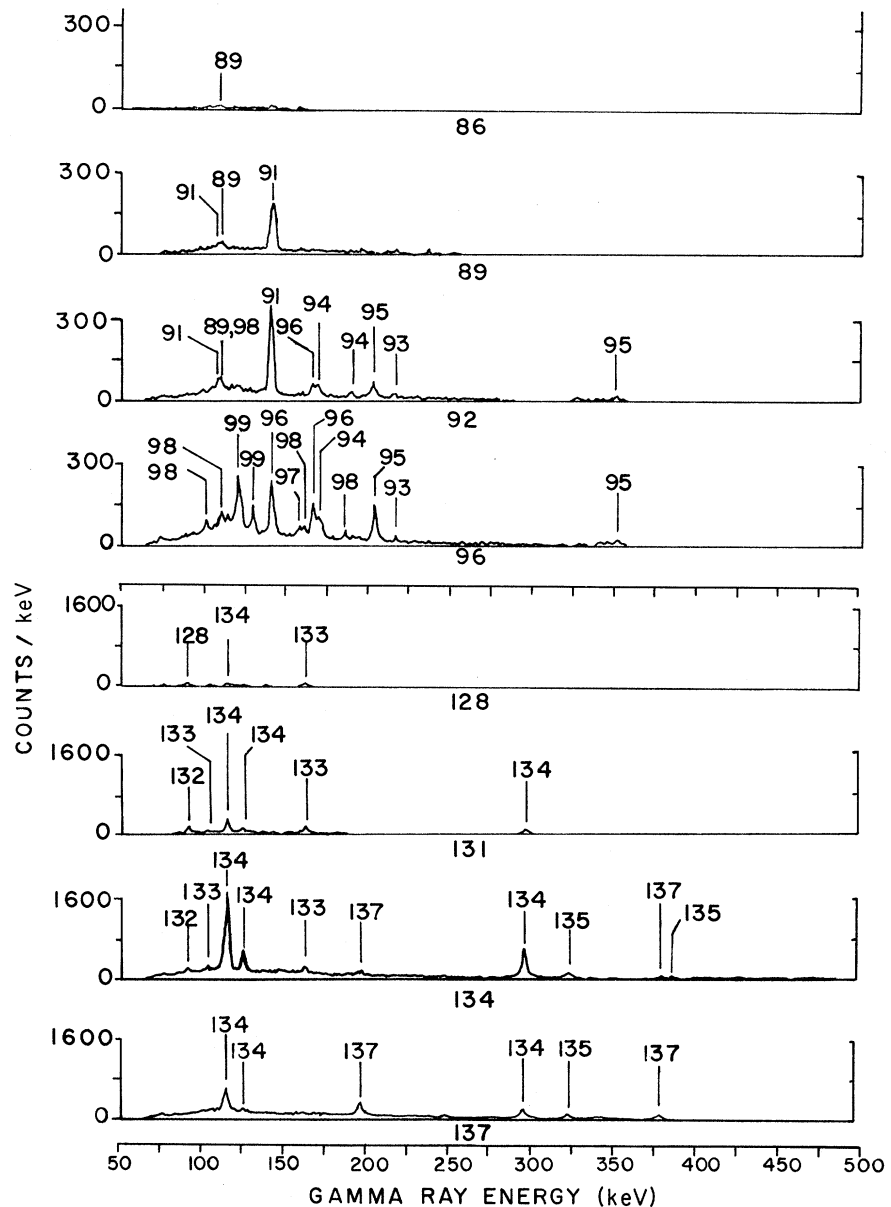
FIG. 6. Examples of γ-ray spectra sorted by fragment mass for the time interval 50 to 2000 nsec after fission. Peaks are labeled by the probable emitting mass. A given peak may appear in more than one spectrum because of the finite experimental mass resolution.

sion and pulse-height defect, was iterated until the change in the mass was less than 0.05 mass units.

For the present experiment we are interested primarily in the post-neutron-emission mass. A check of the procedure used to derive the mass may be obtained by comparing the mass distribution from our two-parameter calibration runs with the radiochemical data of Nervik.[16] As can be seen in Fig. 4 the agreement is reasonable. The largest differences are for masses 112, 115, and for the masses produced by symmetric fission. The agreement with radiochemical data indicates that for present purposes it is probably unnecessary to attempt to unfold the experimental resolution.

B.   Search for γ-Ray Peaks

The total γ-ray spectrum is quite complex (Fig. 5). In order to facilitate a preliminary examination of the spectra, the events were sorted according to mass and into three major time intervals. Examples of the sorted spectra are shown in Fig. 6. It can be seen that γ-ray peaks are well resolved. A computer search for γ-ray peaks was made by fitting the spectra with Fourier series. The series were cut off when the structure in the
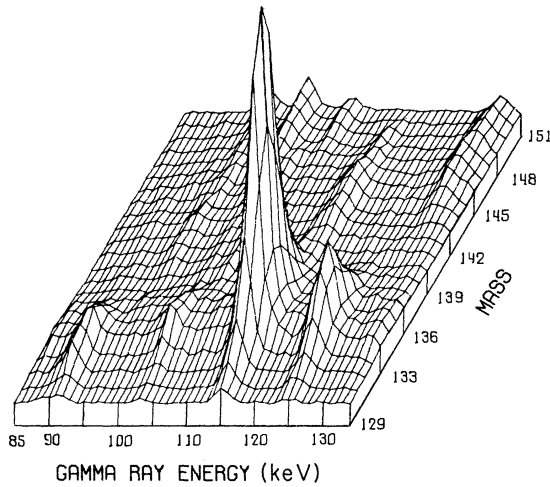
FIG. 7. Isometric plot of counts versus γ-ray energy and mass number of the emitting fragment for the time interval of 50 to 500 nsec after fission.

curves was comparable to the experimental resolution. The smoothed spectra for each mass and time interval were then analyzed for peaks. The list of peaks was then further screened manually, using various criteria; for example, that each γ-ray peak appear in the spectra for adjacent masses (owing to finite mass resolution).

C. Analysis of Individual γ Rays

Each γ ray located in the preliminary search described above was subjected to a multiparameter analysis. A window of ΔE_γ, ΔM, and Δt was set

around the peak. The window was chosen to optimize the separation of the peak from other nearby peaks and for maximum signal-to-background ratio. The adjustment of the window was done by trial and error. The counts in the window were then summed over Δt to obtain a three-dimensional array of counts versus E_γ and M.

A nonlinear least-squares fit to the data was then made using a Gaussian distribution in both E_γ and M (a bivariate normal distribution) plus a background represented by a function containing adjustable parameters. The background parameters were determined with windows set adjacent to the peak. In some cases where this procedure was unsuccessful, the variation of the background with mass was simply assumed to follow the mass-yield curve. The completed fit to the data peak yielded E_γ, the mass, the integrated number of counts (volume) under the peak, and the statistical standard deviations of these quantities.

As an illustration of the analysis, we show in Fig. 7 an isometric plot of the data showing two large peaks and several smaller ones in the mass region 129 to 151 and E_γ region 85 to 134 keV. For the large peak (115.0 keV, mass 134), slices taken through the three dimensional peak along planes of constant integral mass are displayed in Fig. 8.

In order to determine the time dependence of the γ ray in question the window in ΔM and ΔE_γ was narrowed around the peak. The time dependence was fitted with a sum of up to three exponentials with different half-lives and a constant term. The decay curve for the 115.0-keV γ ray from mass 134 is shown in Fig. 9.
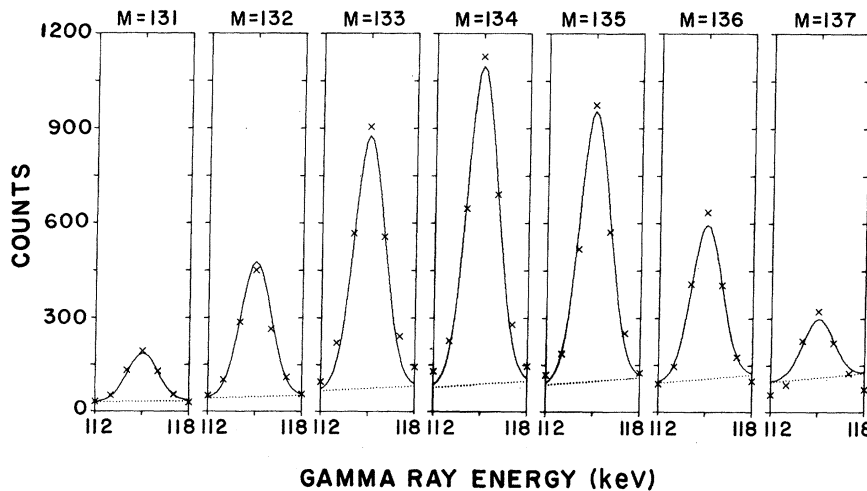
FIG. 8. Mass and γ-ray energy distribution for the 115.0-keV γ ray from mass 134. The crosses are experimental data and the solid line a fitted bivariate normal distribution in mass and γ-ray energy. The dotted line is a background function. The graphs are cross sections taken at integral masses through the three-dimensional peak (see Fig. 7). The fit yielded the following data: γ-ray energy, 115.0 keV, FWHM 2.3 keV; most probable mass 134.1, FWHM 3.7; counts in peak 9865 ± 296.

TABLE I. Delayed γ rays from spontaneous fission of ^{252}Cf.

E_γ (keV)	Mass; ΔM	Photons/ fragment	Photons/fission; error (%)	$t_{1/2}$ (nsec)	Remarks
102.0	$82+3,-1$	0.03	$0.000\,015\pm35$	35	E_γ error: ±0.3 keV.
111.2	89 ± 0	0.05	$0.000\,20\pm20$	3000	Intensity and half-life are estimated.
108.8	91 ± 0	0.15	$0.000\,88\pm8$	25 ⌐	
117.1	$91+0,-1$	0.02	$0.000\,12\pm17$	19 ⌐	Small mass FWHM, 1.7 units.
142.0	$91+1,-0$	0.62	0.0036 ± 7	55	
237.8	91 ± 1	0.046	$0.000\,27\pm16$	9 ⌐	
276.5	$91+1,-0$	0.075	$0.000\,43\pm13$	6 ⌐	
217.2	93 ± 0	0.058	$0.000\,44\pm10$	70 ⌐	
169.8	94 ± 1	0.032	$0.000\,30\pm30$	440 ¦	
191.1	$94\pm0,-1$	0.030	$0.000\,29\pm13$	110 ⌐	
204.3	95 ± 2	0.54	0.0062 ± 12	24 ⌐	Large mass FWHM, 7.0 units; probably two interfering lines.
352.3	95 ± 0	0.40	0.0046 ± 7	21 ⌐	
140.9	$96+1,-0$	0.062	$0.000\,84\pm20$	360 ⌐	
167.1	$96+1,-0$	0.11	0.0015 ± 15	240 ⌐	
158.0	97 ± 1	0.023	$0.000\,39\pm20$	1500 ⌐	Large mass FWHM, 6.1 units.
100.7	$98+0,-1$	0.016	$0.000\,33\pm11$	530	
111.0	98 ± 0	0.018	$0.000\,38\pm15$	760	
161.2	$98+1,-0$	0.064	$0.001\,34\pm11$	68	
170.5	98 ± 0	0.094	0.0020 ± 21	1100	
186.4	98 ± 1	0.024	$0.000\,50\pm13$	650	
204.0	98 ± 1	0.061	0.0013 ± 11	3000	Intensity and half-life are estimated.
229.0	98 ± 0	0.035	$0.000\,74\pm11$	6	
121.4	$99+1,-0$	0.19	0.0048 ± 10	360 ⌐	
122.0	$99+1,-0$	0.098	0.0025 ± 9	22	
129.8	$99+1,-0$	0.11	0.0029 ± 15	340	
415.6	$99+1,-0$	0.020	$0.000\,51\pm22$	16	
143.0	100 ± 2	0.05	0.0015 ± 50	10 ⌐	Cannot resolve this line. Values are estimated.
213.3	100 ± 0	0.021	$0.000\,62\pm15$	7 ⌐	
426.8	100 ± 1	0.029	$0.000\,88\pm22$	16	Large mass FWHM, 6.3 units.
614.2	100 ± 0	0.11	0.0034 ± 9	20	
91.5	$101+0,-1$	0.021	$0.000\,76\pm10$	19 ⌐	
98.3	$101+1,-0$	0.019	$0.000\,67\pm22$	21 ⌐	
152.1	$101+1,-0$	0.10	0.0037 ± 8	7	
180.5	$102+1,-0$	0.013	$0.000\,55\pm10$	86	
164.2	103 ± 0	0.059	0.0028 ± 8	8	
112.3	104 ± 0	0.0061	$0.000\,35\pm18$	15	
140.9	104 ± 0	0.028	0.0016 ± 9	62	
144.1	104 ± 1	0.040	0.0023 ± 34	7 ⌐	Large γ ray FWHM, 4.0 keV; may be Doppler shifted from 139 keV.
238.9	104 ± 0	0.18	0.010 ± 14	5 ⌐	Large γ ray FWHM, 3.7 keV; may be Doppler shifted from 231 keV.
251.6	$104+1,-0$	0.066	0.0037 ± 9	4 ⌐	
85.6	$105+1,-0$	0.018	0.0012 ± 24	16 ⌐	
102.8	105 ± 0	0.059	0.0038 ± 11	15 ⌐	
193.6	105 ± 0	0.038	0.0024 ± 15	5	Large γ ray FWHM, 5.1 keV; may be Doppler shifted from 188 keV.
205.0	$105+1,-0$	0.0085	$0.000\,54\pm14$	9	Small mass FWHM, 2.8 units.
172.2	106 ± 0	0.082	0.0054 ± 11	5	

TABLE I (*Continued*)

E_γ (keV)	Mass; ΔM	Photons/ fragment	Photons/fission; error (%)	$t_{1/2}$ (nsec)	Remarks
66.2	108 + 0, −1	0.10	0.0060 ± 10	140 ⌝	
86.3	108 + 1, −0	0.092	0.0054 ± 27	140 ⌝	
90.0	108 + 1, −0	0.037	0.0022 ± 18	120 ⌝	
90.2	108 ± 0	0.022	0.0013 ± 36	⌐ 15	
105.8	108 ± 0	0.015	0.000 91 ± 9	120 ⌐	
119.2	108 ± 0	0.011	0.000 62 ± 18	110 ⌐	
134.6	108 ± 0	0.0030	0.000 18 ± 21	100 ⌐	Small mass FWHM, 2.7 units.
153.6	108 ± 0	0.13	0.0077 ± 7	110 ⌐	
176.2	108 + 1, −0	0.052	0.0031 ± 7	110 ⌐	
250.0	108 ± 0	0.018	0.001 07 ± 10	⌐ 16	
115.6	109 ± 0	0.0078	0.000 45 ± 20	18 ⌝	
119.4	109 ± 0	0.023	0.0014 ± 29	16 ⌝	Large γ ray FWHM, 4.0 keV.
210.1	109 + 1, −0	0.0017	0.000 098 ± 22	120 ⌝	Small mass FWHM, 2.4 units.
60.3	110 + 0, −1	0.078	0.0045 ± 41	210 ⌝	
96.2	110 ± 0	0.14	0.0080 ± 7	550	
131.8	110 ± 0	0.030	0.0017 ± 17	11 ⌝	
222.5	110 ± 0	0.037	0.0021 ± 8	8 ⌝	
239.9	110 + 0, −1	0.025	0.0014 ± 20	3	Large γ ray FWHM, 3.9 keV; may be Doppler shifted from 233 keV.
103.5	111 + 0, −1	0.11	0.0059 ± 8	14	
150.5	111 ± 0	0.14	0.0080 ± 7	6 ⌝	
167.1	111 + 1, −0	0.026	0.001 43 ± 10	5 ⌝	
225.7	111 + 0, −1	0.013	0.000 72 ± 15	1500	
60.5	112 ± 1	0.12	0.0061 ± 15	24	
189.5	112 ± 0	0.014	0.000 70 ± 15	7 ⌝	
154.6	113 ± 1	0.025	0.0010 ± 42	8 ⌝	
212.3	113 ± 0	0.012	0.000 49 ± 15	5 ⌝	
304.3	113 ± 0	0.035	0.001 44 ± 13	5 ⌝	
84.9	115 + 0, −1	0.059	0.0019 ± 25	61	Small mass FWHM, 2.5 units.
128.9	116 ± 0	0.029	0.000 84 ± 10	12 ⌝	
174.4	116 + 1, −0	0.0095	0.000 27 ± 12	9 ⌝	Small mass FWHM, 2.4 units.
222.3	116 ± 0	0.013	0.000 39 ± 11	6 ⌝	Small mass FWHM, 2.8 units.
91.3	117 + 0, −1	0.0049	0.000 105 ± 15	14 ⌝	Small mass FWHM, 2.0 units.
90.5	122 ± 0	0.011	0.000 026 ± 26	7	Small mass FWHM, 1.0 units.
89.7	128 ± 0	0.06	0.000 24 ± 25	53 ⌝	
120.6	128 ± 4	0.05	0.000 19 ± 42	21	Cannot resolve mass.
137.8	129 + 1, −0	0.034	0.000 17 ± 10	52 ⌝	
96.5	130 ± 0	0.024	0.000 20 ± 21	2100	
91.2	132 ± 0	0.037	0.000 75 ± 11	120 ⌝	
375.4	132 + 2, −0	0.016	0.000 32 ± 21	⌐ 8	
85.7	133 + 0, −1	0.083	0.0026 ± 21	⌐ 12	
103.3	133 ± 0	0.012	0.000 37 ± 9	130 ⌝	
163.0	133 + 0, −1	0.055	0.0018 ± 8	110 ⌝	
59.9	134 ± 0	0.069	0.0027 ± 20	130 ⌝	
115.0	134 ± 0	0.16	0.0061 ± 7	162 ⌝	
125.1	134 ± 0	0.045	0.001 76 ± 7	115	
182.4	134 ± 0	0.031	0.0012 ± 10	15	
296.9	134 ± 0	0.27	0.0103 ± 7	162	
1151.6	134 + 0, −1	0.055	0.0021 ± 11	90	
1279.8	134 ± 0	0.32	0.0126 ± 9	164 ⌝	
324.5	135 ± 0	0.073	0.0031 ± 8	570 ⌝	

TABLE I (*Continued*)

E_γ (keV)	Mass; ΔM	Photons/ fragment	Photons/fission; error (%)	$t_{1/2}$ (nsec)	Remarks
387.1	135 + 0, −1	0.019	0.000 82 ± 21	−110	
1181.0	135 + 0, −1	0.070	0.0030 ± 13	670	
261.1	136 + 0, −1	0.037	0.0017 ± 15	4	Large γ ray FWHM, 4.3 keV; may be Doppler shifted from 257 keV.
288.5	136 + 0, −1	0.061	0.0028 ± 9	3	
155.0	137 ± 0	0.026	0.001 27 ± 9	7	
197.3	137 ± 0	0.12	0.0060 ± 8	2800	
380.7	137 ± 1	0.15	0.0073 ± 8	3400	
1221.0	137 + 2, −1	0.15	0.0073 ± 17	6	Large γ ray FWHM, 7.4 keV.
1313.3	137 + 2, −1	0.12	0.0057 ± 24	3000	Intensity and half-life are estimated.
314.4	138 + 0, −1	0.076	0.0039 ± 8	9	
400.2	138 + 0, −1	0.071	0.0037 ± 9	9	
219.4	140 ± 0	0.015	0.000 89 ± 14	4	
103.5	141 ± 2	0.04	0.0023 ± 50	20	See footnote.[a]
90.5	142 ± 0	0.015	0.000 89 ± 14	15	
97.0	142 ± 0	0.047	0.0029 ± 10	16	
106.0	142 ± 2	0.04	0.0023 ± 50	20	See footnote.[a]
117.3	144 ± 1	0.23	0.0133 ± 9	14	Large mass FWHM, 6.8 units; probably two interfering lines.
109.7	145 ± 2	0.04	0.0023 ± 50	20	See footnote.[a]
183.5	145 ± 1	0.026	0.0014 ± 12	6	Large γ ray FWHM, 4.8 keV; may be Doppler shifted from 179 keV.
341.0	145 ± 1	0.012	0.000 65 ± 15	−20	
82.8	146 + 1, −0	0.14	0.0069 ± 18	13	
105.0	146 ± 2	0.05	0.0023 ± 50	20	See footnote.[a]
130.5	146 ± 0	0.066	0.0032 ± 14	19	
167.7	146 + 1, −0	0.15	0.0073 ± 7	13	
251.1	146 ± 0	0.012	0.000 59 ± 13	6	
288.2	146 ± 0	0.060	0.0029 ± 15	17	
364.2	146 ± 0	0.032	0.001 55 ± 11	11	
58.3	147 ± 2	0.19	0.0078 ± 11	8	Large mass FWHM, 7.7 units; may be two interfering lines.
158.8	147 + 0, −1	0.075	0.0030 ± 10	10	
283.9	147 + 1, −0	0.16	0.0064 ± 9	8	
445.0	147 ± 1	0.018	0.000 73 ± 40	14	Large mass FWHM, 6.6 units; may be two interfering lines.
135.4	148 + 1, −0	0.22	0.0076 ± 9	9	Large γ ray FWHM, 5.9 keV; may be Doppler shifted from 132 keV.
142.6	149 + 0, −1	0.074	0.0021 ± 15	9	
97.5	150 ± 1	0.078	0.0019 ± 8	18	
103.2	150 + 0, −1	0.046	0.0011 ± 27	200	
109.4	150 ± 0	0.014	0.000 32 ± 16	67	
130.9	150 ± 0	0.023	0.000 54 ± 9	160	
163.5	152 ± 0	0.0074	0.000 114 ± 22	82	Small mass FWHM, 2.5 units.
247.4	152 + 0, −1	0.011	0.000 17 ± 19	72	
141.7	153 ± 0	0.071	0.000 91 ± 10	1400	
191.6	153 ± 0	0.11	0.001 35 ± 16	850	
162.5	154 + 1, −0	0.057	0.000 62 ± 21	2100	
169.9	154 ± 0	0.014	0.000 15 ± 19	1700	Small mass FWHM, 1.6 units.
167.1	156 + 1, −0	0.038	0.000 25 ± 12	77	
174.2	156 ± 0	0.019	0.000 126 ± 11	88	Small mass FWHM, 1.7 units.

TABLE I *(Continued)*

E_γ (keV)	Mass; ΔM	Photons/ fragment	Photons/fission; error (%)	$t_{1/2}$ (nsec)	Remarks
267.1	156 + 1	0.040	0.000 26 ± 21	185 ⌐	Large γ ray FWHM, 6.6 keV; may be doublet.
243.4	158 + 0, −1	0.029	0.000 10 ± 14	216 ⌐	Small mass FWHM, 2.8 units.
168.2	163 ± 2	0.079	0.000 063 ± 15	1500 ⌐	
152.3	164 ± 2	0.077	0.000 038 ± 17	800 ⌐	

[a]These lines are too close in mass and γ-ray energy to resolve from each other. The only value that could be determined with any accuracy was the total photons per fission (0.010 ±20%) from all four lines. γ-ray energies and mass assignments are estimated.

For each γ ray the intensity per fission and the intensity per fission fragment were calculated from the number of counts under the peak and half-life.

D. Experimental Results

The results of the data analysis are listed in Table I. The γ-ray energies are believed to be uncertain by ±0.2 keV, principally from uncertainty in calibration. For each γ ray the most probable mass of the associated fission fragment is given as well as ΔM, the estimated maximum uncertainty in this assignment. ΔM was given the value zero when the most probable mass fell within 0.2 of an integral number of mass units, and the data were fitted by a Gaussian of less than 6 mass units FWHM. Otherwise ΔM was estimated from the fit and the probable error in the correction for neutron emission in that mass region. The average FWHM of the mass fits was 4.5 mass units; lines relatively isolated in energy and mass had a FWHM of 3.5 to 4.5 mass units. Lines which had FWHM's outside

FIG. 9. Time distribution of the data (crosses) and fitted decay curve (162-nsec half-life) for the 115.0-keV γ ray from mass 134.

the range from 3 to 6 mass units are indicated by comments in Table I.

Intensities are given in terms of photons/fragment and photons/fission. The error in the latter is given as standard deviation in %. The error includes the error from the fit for that particular γ ray and ±6.5% error common to all the γ rays from the absolute calibration. For γ rays with half-lives less than 5 nsec or greater than 2000 nsec considerable uncertainty was introduced into the intensity calculation by the half-life determination, since for very short half-lives the system response influenced the measurement and for long half-lives the decay could not be fitted over a sufficient range. The values for normalized intensity per fragment also depend upon the mass-yield curve. Errors from this source may be large for fragments of low fission yield.

The half-life is given for each γ ray. It is difficult to assign meaningful errors to the half-lives. However, in most cases the % error in the half-life is estimated to be roughly the same as the listed % error in the intensity. For a given mass, those half-lives which are probably the same are connected by solid lines. These γ-ray transitions are presumably members of a cascade fed from the same isomeric state. Lines which are possibly members of such a cascade (but with less certainty because of discrepancies in measured half-lives or mass assignment) are connected with dashed lines.

In Table I a few of the lines are noted as having large γ ray FWHM. Some of these lines have apparent half-lives about the same as the system time response and may be very short (or the order of 1 nsec) half-life transitions seen by the γ-ray detector while the fragments were in flight. If this is the case, the half-life and intensity calculations are in error. An approximate correction for Doppler shift of the γ-ray energy has been made by assuming that the fragments were seen just as they emerged from behind the γ-ray shield. The corrected energy is given in the comments.
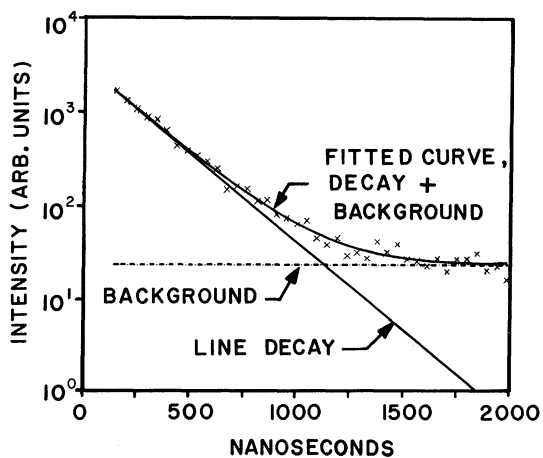
IV. DISCUSSION

A. Systematics of Isomers; Mass Dependence

Examination of Table I shows that delayed γ rays were seen for most fragment masses. Of the 83 masses spanned by the measurements, only 30 are missing from the table. Further, 20 of the missing fragment masses have fission yields of less than 1%, which could account for their absence. Approximately half of the masses have more than one isomeric state populated. These are not necessarily from the same isotope, since each fragment mass includes several isotopes of different atomic number which are potential delayed γ-ray emitters. From an estimate of the total number of isotopes formed with sufficient yield to be observed we conclude that about 50% of the isotopes had isomeric states.

In Fig. 10 the observed isomers are plotted versus Z and A, where Z is the most probable atomic number. For comparison, the known isomers in the same time range as the present measurements are plotted from a compilation.[17] The plot illustrates that the fission-fragment isomers occur in a neutron-rich region of the isotope chart which has not been investigated for isomerism before, and that the number of isomers (between 80 and 100) observed in the present experiment is comparatively large, i.e., that the fission reaction is a copious source of isomers. It can also be seen that neither the fission product isomers or the data for other nuclei show any preference for the "islands of isomerism" which occur prior to the closing of a major shell. These islands are associated with much longer-lived isomers than the present data cover.

In Fig. 11 we display the number of photons per fission versus E_γ for the time interval 10–2000 nsec, synthesized from Table I. The photon spectrum is seen to be rich at low energies with, however, a high-energy group at 1200–1300 keV. In Fig. 12(a) the number of photons per fission is
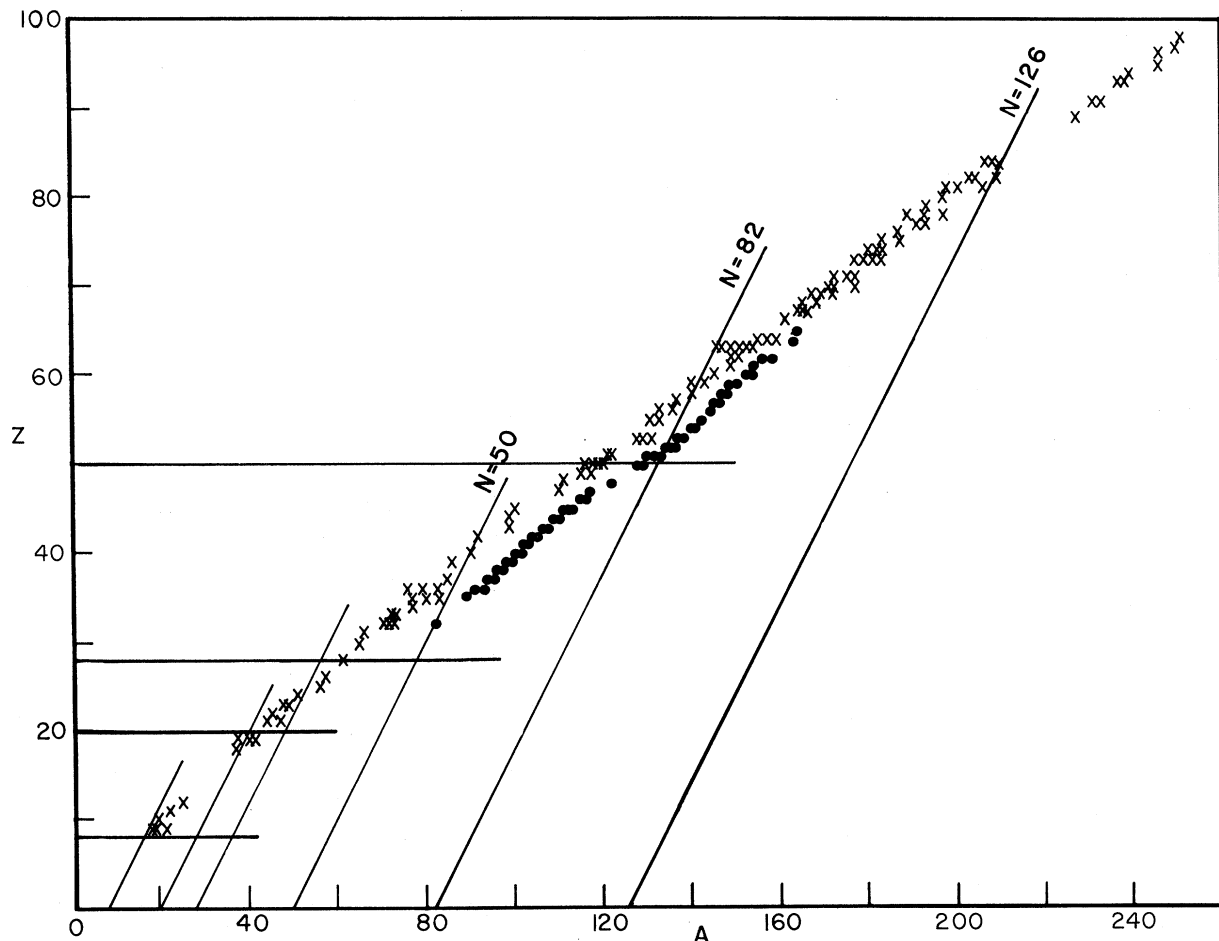
FIG. 10. Plot of the known isomers versus Z and A for half-lives from 3 to 3000 nsec. The crosses are taken from the compilation by Kantele and Tannila (see Ref. 17). The dots are from the present work on fission fragments; the isomers are assigned the most probable Z. Many of the dots represent more than one isomer.
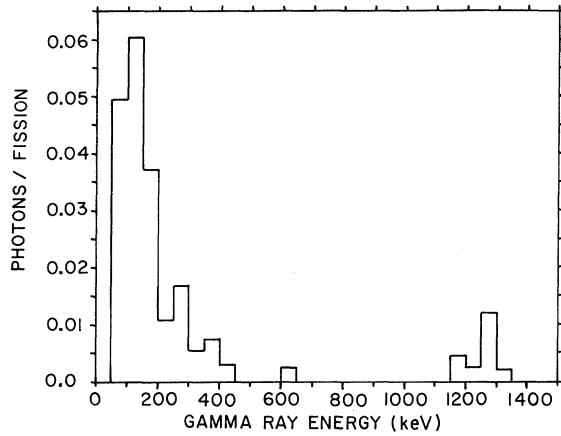
FIG. 11. Energy spectrum of delayed fission γ rays for the time interval 10–2000 nsec after fission. The spectrum is derived from the analyzed results in Table I.

plotted versus fragment mass for the time interval 10–2000 nsec. This figure shows that while delayed γ rays occur for most masses, the photon intensity is concentrated on certain masses, notably 91, 96, 99, 108, and 110 on the light-mass peak,

plus 134, 137, and 146 on the heavy-mass peak. Figure 12(b) is similar to Fig. 12(a) except that energy per fission is plotted in place of photon number. The concentration of energy at masses 134 and 137 is striking. The group of high-energy transitions noted in Fig. 11 comes from these two masses.

Figures 13(a)–(c) display the number of photons per *fission fragment* versus fragment mass for three successive time intervals. The changes in the relative intensities arising from the different

FIG. 12. (a) Photon intensity versus fragment mass for the 10- to 2000-nsec time interval. (b) Energy intensity versus fragment mass for the 10- to 2000-nsec time interval.
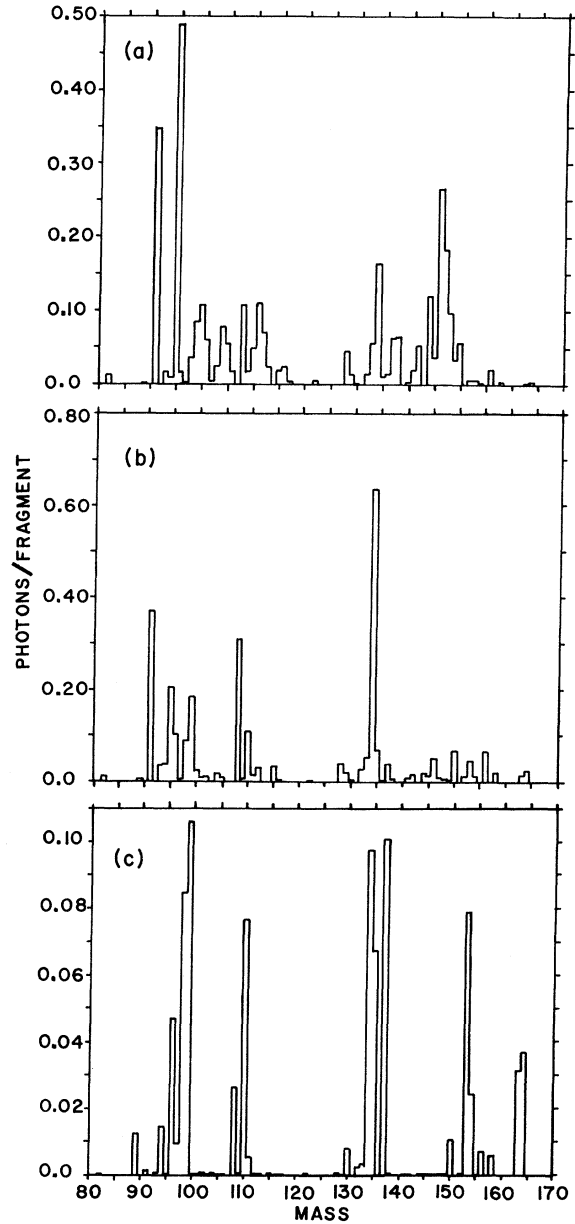
FIG. 13. Photons/fragment versus mass for three time intervals: (a) 10 to 50 nsec, (b) 50 to 500 nsec, (c) 500 to 2000 nsec.

half-lives are apparent. Also, it can be seen that
the γ rays are grouped roughly into four mass re-
gions centered about masses 96, 108, 134, and
146. Practically no delayed γ rays come from the
minima near masses 102 and 139 in spite of the
high yields of these fragments. [See also Figs.
12(a), (b).] This grouping of the yields into four
mass regions was noted by Johansson,[5] who sug-
gested that the peaks near masses 96 and 108 are
associated with two regions of deformed nuclei
separated by the semimagic proton number 40,
which occurs near mass 101. Similarly, the peak
near mass 146 is supposed to be associated with an
extension of the already known deformed region in
the rare earths. It was further suggested that the
peak at mass 134 (Johansson designated it approxi-
mately mass 132) could be related to the magic pro-
ton number 50 and magic neutron number 82.

In connection with the maxima in delayed γ-ray
yield at certain masses, we have pointed out[18] that
the data of Johansson[1] for *prompt* γ-ray yields
show dips at the corresponding masses. This is
particularly evident at masses 108 and 134. The
correlation between prompt and delayed yields
suggests that the occurrence of delayed transitions
simply subtracts radiation from the prompt yield,
i.e., that the total yield as a function of mass is a
relatively smooth sawtooth curve. Albinsson and
Lindow[19] have observed similar effects in the
yield of prompt γ rays from slow neutron induced
fission of ^{235}U.

B. Multipolarities of Transitions

In Fig. 14 the half-lives of the γ rays are plotted
versus E_γ. For comparison the single-particle
transition rates are shown for $E1$, $E2$, and $E3$
transitions. From the present data there is no di-
rect knowledge of whether a given γ ray was a
transition from the isomeric state or a lower mem-
ber of a cascade. However, over most of the plot
an appreciable fraction of the points do represent
direct transitions. Therefore, we can discuss the
bulk of the data as to multipolarities.

It is concluded that most of the transitions are
$E1$ or $E2$ with probably some $M1$ transitions pres-
ent. The occurrence of $E1$ transitions over the en-
tire range of the data would imply hindrance fac-
tors from 10^{-5} to 10^{-8} compared with the Weisskopf
estimate. Such factors are commonly encountered.[20]
Over the faster half of the range, i.e., hindrances
of 10^{-5} to 5×10^{-7}, all types of nuclei can contrib-
ute: spherical, deformed, even A, and odd A.
Over the slower half, for hindrances of 5×10^{-7} to
10^{-8}, K-forbidden transitions in deformed nuclei,
either odd or even A, are to be expected. A $|\Delta K|$
of 2 or 3 would be sufficient to account for the
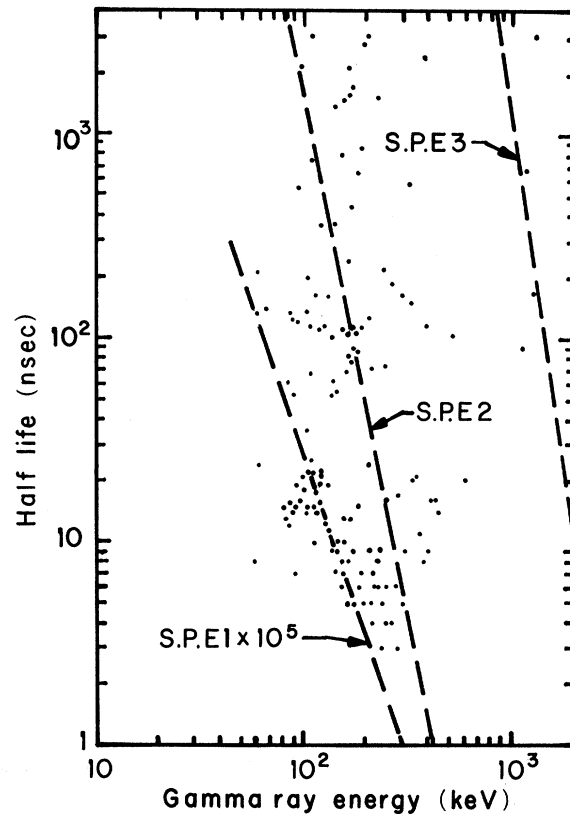
FIG. 14. Half-lives of the γ rays versus γ-ray energy.
The lines show single-particle transition rates for com-
parison.

hindrance factors.

Likewise the entire range of the data is spanned
by typical $E2$ transition rates.[21] Points lying be-
low the $E2$ single-particle line are within the en-
hancement factors of up to 10^2 observed in transi-
tions between collective states, particularly rota-
tional states in deformed nuclei. Points near the
$E2$ line or above could be $E2$ transitions with ΔK
values of 2 to 4. Fairly pure single-particle con-
figurations can also give transition rates above the
single-particle line.

$E3$ transitions seem to be excluded for the bulk
of the data, since experimentally observed $E3$
rates are usually hindered by more than an order
of magnitude over the single-particle rate. There
are only a few points, for $E_\gamma > 10^3$ keV, which are
near the $E3$ line. One of these, the 1280-keV γ ray
from mass 134, is believed to be a lower member
of a cascade. It is not possible to say more about
the others.

To summarize, it appears that the fission-frag-
ment isomers observed in the present experiment
can be accounted for by $E1$ and $E2$ transitions of
the sort encountered in isomers nearer the line of

stability. This suggests that the initially high spins (8–10 $\hbar$) of the fragments play a lesser role in determining the character of the delayed γ rays than previously thought.[5] This conclusion is reinforced by the observation that for most of the fragments the isomeric states are populated in only a small fraction of the deexcitations. Furthermore, we do not have any evidence of transitions to high members of ground-state rotational bands. There are on the average approximately four prompt γ rays per fragment; these can reduce the spin considerably. Finally, one would expect the odd-odd and odd-A nuclei to have low-lying isomeric states which can be easily populated. We should point out that this discussion has dealt with the characteristics of all the isomers observed. On the other hand, there are a few isomers which account for most of the intensity. These nuclei evidently have atypical level schemes which result in an unusually high probability of populating the isomeric state.

C. Completeness of Data

For half-lives less than 10 nsec only strong or isolated lines could be analyzed because of the large background from prompt γ rays. Below 80 keV only the strongest lines were analyzed; between 70 and 80 keV no lines were analyzed, because of interference from lead x rays.

We have attempted to assess the extent to which the data in Table I account for the observed counts. The counting rate versus time was synthesized by applying a detector response function to the data of Table I and adding background. Because of difficulties in synthesizing complex spectra, only γ rays above 200 keV were included. At early times there was an excess of actual counting rate over the synthesized, spread over all γ-ray energies, which fitted an 11-nsec half-life. The excess was 75% of the data at 10 nsec. Most of the excess probably came from short-half-life transitions which were not analyzed and from the tail of the prompt γ rays produced by the Ge-detector time response.

The data counting rate was still about 20% greater than the synthesized, out to several hundred nsec. On the light-mass peak the excess had a ~150-nsec half-life and was located in a narrow region around mass 113 and a broader region near mass 96 or 97. The excess counts decreased smoothly from 200 to 1500 keV and did not resemble the spectrum from one or a few high-energy γ rays. A similar but much weaker excess was associated with masses near 153. It is curious that the excess of counts should be associated with certain mass regions. Perhaps it results from a near continuum of γ rays just below the limit of detectability as individual peaks. At any rate, we esti-

mate that the total γ-ray energy from unresolved lines is at most 20% of that of the resolved lines for $200 < E_\gamma < 2000$ keV and $t < 100$ nsec.

D. Detailed Features of Data

1. γ Rays from Mass 134

It was noted in Sec. IV A that the delayed γ rays from mass 134 are exceptionally intense and include high-energy transitions. The mass distributions for the γ rays gave 134 consistently, and not 132 which includes doubly magic ^{132}Sn. The most probable charge for mass 134 is estimated to be 52; the corresponding neutron number is then 82. The energies of the first 2+ states for nuclei having $N = 82$ and $Z = 54$, 56, and 58 were extrapolated to $Z = 52$ to predict that ^{134}Te will have a 2+ state at 1.28 MeV. The theoretical calculation of Kisslinger and Sorensen[22] predicted a collective vibrational state at about 1.3 MeV. It is therefore likely that the intense 1279.8-keV γ ray from mass 134 is from the 2+ to 0+ transition in ^{134}Te. The assignment of the 162-nsec isomer to Te is further supported by x-ray measurements by the Argonne group.[23] They found a 200-nsec Te K x ray from mass-134 fission fragments.

There are two other mass-134 γ rays with the same half-life (162 nsec) as the 1279.8-keV γ ray, with energies of 115.0 and 296.9 keV. When the intensity of the 115.0-keV line is corrected for internal conversion assuming an $E2$ transition, the result is 0.28 photons/fragment. The data are then consistent with the series cascade shown in Fig. 15. It should be noted that an intensity of 0.28 photons per fragment of mass 134 implies more than 0.6 photons per ^{134}Te fragment, depending on the charge distribution of mass-134 fragments. Kisslinger and Sorensen[22] found that the $(g_{7/2})^2$ quasiparticle levels should be near the collective 2+ level. These quasiparticle levels might then feed the 2+ level by low-energy transitions. It would be desirable to have a shell-model calculation of the levels of ^{134}Te.

The 59.9-keV line has a half-life of 132 nsec with an uncertainty which allows the transition to be grouped with either the 162-nsec cascade or the ~109-nsec cascade. However, evidence is given below in Sec. 4 that the 59.9-keV γ ray is associated with I and not Te. Therefore, the ~109-nsec cascade is probably from ^{134}I. The 59.9-keV transition can only be $E1$ or $M1$, since the intensity, when corrected for internal conversion, would imply a fission yield much too large for the emitting isotope in the case of $E2$ or higher multipoles.

2. γ Rays from Mass 137

The γ rays from mass 137 are noteworthy in that

$T_{1/2}$= 162 nsec

115.0 keV, (E2), 0.28 γ/Frag

296.9 keV
0.27 γ/Frag

(2+)

1279.0 keV
(E2), 0.32 γ/Frag

0+

$^{134}_{52}$Te$_{82}$
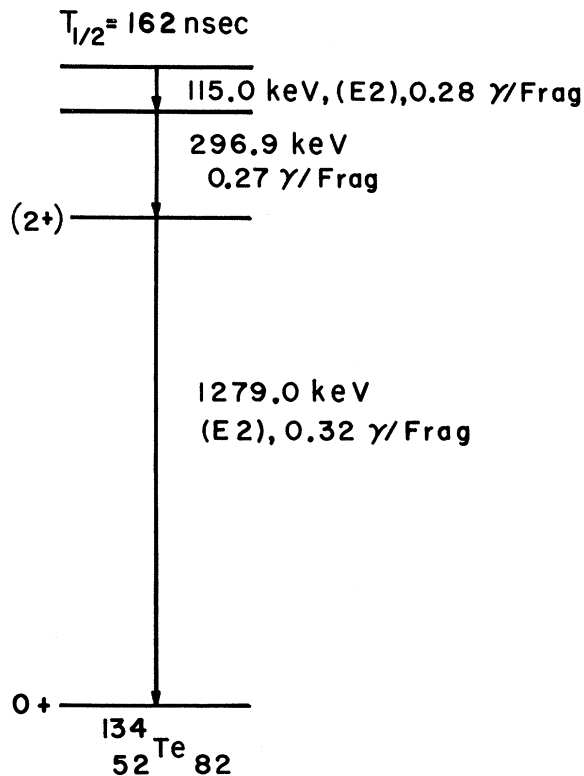
FIG. 15. Suggested decay scheme for the 162-nsec isomer in mass 134. The order of the 115.0- and 296.9-keV transitions is undertermined.

they include three 3000-nsec lines of fairly strong intensity and, like mass 134, include high-energy γ rays. The intensities of the 197.3-, 380.7-, and 1313.3-keV lines are consistent with a series cascade from a ~3-μsec isomeric state. This isomeric state is probably that observed by Walton and Sund[7] in neutron-induced fission of ^{239}Pu and ^{235}U. The energies found by Walton and Sund with a NaI detector were systematically slightly higher, but the differences are probably within the errors. The assignment of this isomer to mass 137 (or to mass 136, see below) would explain the occurrence of the same isomer with comparable yield in the fission of ^{252}Cf, ^{239}Pu, and ^{235}U.

It must be noted, however, that ^{136}Xe has a set of cascade γ rays with energies close to those observed here. Lundan and Süvola[24] have reported a cascade of γ rays with energies of 197.7±0.3, 381.7±0.2, and 1313.2±0.8 keV among the γ rays emitted following β^- decay of ^{136}I. They also report a 1320.2±1.0-keV γ ray and place it in the cascade between the 381.7- and 1313.2-keV transitions. In earlier low-resolution work Johnson and O'Kelley[25] reported similar results. We have examined our data for a 1320-keV line but do not find it. If it were present in the cascade its intensity

would, of course, have been equal to that of the 1313-keV line.

This difficulty is apparently removed by a new direct determination of the level sequence in ^{136}Xe by proton inelastic scattering carried out by Moore et al.[26] They report levels at 1.30, 1.68, 1.89 MeV, and higher. The cascade observed in the present experiment fits into this sequence quite well, as shown in Fig. 16. The agreement leaves little doubt that our cascade comes from ^{136}Xe. We conclude that the earlier proposed decay schemes were incomplete and possibly incorrect.

The identification with ^{136}Xe means that our initial mass assignment was incorrect by one mass unit. This could have arisen from "fine structure" in $\bar{\nu}$ as a function of mass. The 83rd neutron would be loosely bound. Furthermore, the data on which our neutron correction was based were taken with fairly coarse mass resolution. $^{136}_{54}$Xe$_{82}$ is next to $^{134}_{52}$Te$_{82}$ in the sequence of even-even nuclei with 82 neutrons. This explains the similarity between the isomeric states and the γ cascades in the two nuclei.

$T_{1/2}$= 3000 nsec

197.3 keV
0.12 γ/Frag

380.7 keV
0.15 γ/Frag

2+

1313.3 keV
0.12 γ/Frag

0+

$^{136}_{54}$Xe$_{82}$
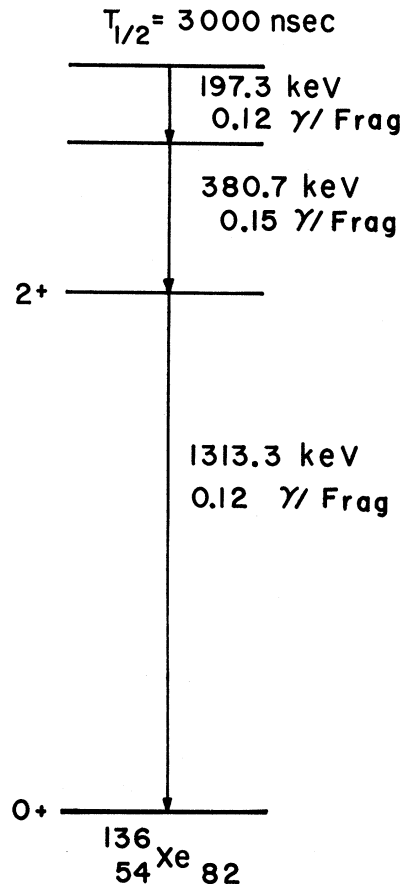
FIG. 16. Suggested decay scheme for the 3000-nsec isomer identified with ^{136}Xe.

3. Search for Rotational Bands

The present data have been examined for rotational cascades. No case was found of a cascade of at least three γ rays from the same mass, with the same half-life, with the same intensity (corrected for internal conversion if necessary), and which satisfied the relative energy requirements for a rotor. (Less stringent requirements do not lead to conclusive results.) Thus it can be stated that the isomeric states seen in the present work do not populate the high members of a rotational band. Since many of the fission fragments undoubtedly have deformed ground states, it is necessary to explain the absence of rotational bands in the data. A plausible explanation is that the isomeric states are more likely to occur in the low-lying levels of odd-odd or odd-A nuclei than in even-even nuclei. Furthermore, in the absence of feeding from a higher-lying isomeric state the 6+-to-4+ transition, itself in a ground-state rotational band of an even-even nucleus, would be expected to have a half-life of the order of 1 nsec, and hence would not be seen at the longer times we are concerned with.

One of the striking results of the earlier work of Johansson[5] was the occurrence in the γ-ray energy spectrum of a series of peaks associated with $A \sim 152$ and $A \sim 110$, whose energies seemed to be in agreement with those calculated for rotational cascades. However, the present data, after mass sorting, do not exhibit rotational cascades. It appears quite likely that the peaks in Johansson's data were associated with several different fragment masses, even complementary fragment masses. Thus the $A \sim 152$ spectrum can be approximated by γ rays from masses 95, 147, 150, 152, and 153. The $A \sim 110$ spectrum might have included γ rays from masses 110, 113, and 138.

4. Comparison with Other Results

Some of the cascade γ rays observed in the present work, particularly those from low-lying states, should also be present in the prompt γ rays. The Berkeley group[27] has recently compiled the results of multiparameter measurements of prompt (<3 nsec) K x rays, conversion electrons, and γ rays from spontaneous fission of ^{252}Cf. The experiments included mass assignments from fragment kinetic energy measurements. A number of possible identifications with the present work are shown in Table II. This matching allows assignment of the atomic number to the isotope giving the transition, and determines that the γ ray in question did not come directly from the isomeric level.

TABLE II. Comparison of present results on delayed γ rays with data of Watson *et al.* (see Ref. 27) for prompt γ rays ($t_{1/2} < 3$ nsec). Confidence levels for latter data: A, $E_\gamma \pm 1$ keV, ± 1 amu; B, $E_\gamma \pm 5$ keV, ± 2 amu; C, atomic number ± 1 (atomic number exact in A, B).

Present results		Watson *et al.*			
E_γ (keV)	Mass number	E_γ (keV)	Mass number	Atomic number	Confidence level
98.3	101, +1, −0	99	101	40(Zr)	C
152.1	101, +1, −0	153	102	40(Zr)	B
172.2	106, ± 0	172	106	42(Mo)	A
193.6	105, ± 0	192	106	42(Mo)	A
66.2	108, +0, −1	66	107	43(Tc)	C
150.5	111, ± 0	150	110	44(Ru)	A
239.9[a]	110, +0, −1	241	110	44(Ru)	A
59.9	134, ± 0	59	136	53(I)	B
183.5[a]	145, ± 1	183	144	56(Ba)	A
130.5	146, ± 0	131	146	57(La)	A
158.8	147, +0, −1	158	148	58(Ce)	A
142.6	149, +0, −1	143	149	59(Pr)	A
163.5	152, ± 0	163	152	58(Ce)	B

[a] Energy without correction for Doppler shift.

Wilhelmy[28] has made high-resolution measurements of x rays and γ rays which follow β decay of ^{252}Cf fission products. It is to be expected that some of the states involved in the present work will also be populated by the appropriate β decays. A search of the tables reveals a few cases where the γ-ray energy and mass assignments from the two experiments are close. Some caution is necessary, since accidental agreements are likely to occur among the large number of γ rays.

Of some interest is the set of γ rays with energies of 153.8 ± 0.2, 258.3 ± 0.3, and 401.6 ± 0.3 keV ascribed by Wilhelmy to ^{138}Cs. Alvager *et al.*[29] observed γ rays at 154.3 ± 1.5, 258.6 ± 1.5, and 401.5 ± 1.5 from fission fragments with mass 138 using a mass spectrometer. In the present work γ rays were seen at 155.0 ± 0.2 (mass 137), 261.1 ± 0.2 (mass 136), and 400.2 ± 0.2 keV (mass 138), which may be the same set observed in the above experiments, although there is some disagreement in the γ-ray energies and mass assignments. All three of the γ rays had half-lives less than 10 nsec, which is shorter than the optimum range of half-lives for the present experiment. Similarly, Wilhelmy assigned a 218.7 ± 0.2-keV line to ^{139}Cs, and Alvager *et al.* observed a 218.8 ± 1.0-keV γ ray from mass 139. We observed a 219.4-keV γ ray from mass 140 with a 4-nsec half-life. There were a few other possible matches between the present data and that of Wilhelmy or Alvager *et al.* The number of cases is small enough to suggest that the experiments are biased in favor of different types of nuclei.
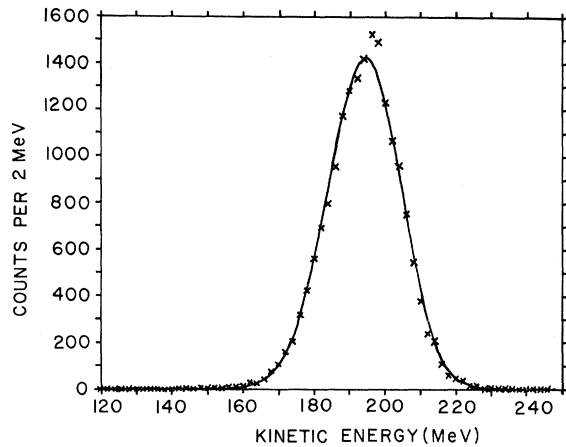
FIG. 17. Distribution of kinetic energy of fissions producing fragments which have postneutron mass 134 and emit 115-keV delayed γ rays.

5. Kinetic Energy Distributions for Fragments Emitting Particular γ Rays

The present data can be sorted to obtain the fragment kinetic energy distribution for events producing a certain γ ray. This corresponds to selecting fission events in which one fragment is left in a given isomeric state; hence that fragment is necessarily always the same isotope. One such distribution is illustrated in Fig. 17. In this case one fragment has a post-neutron-emission mass of 134, and the atomic number is believed to be 52 (see Sec. 1 above).

The curve fitted to the experimental points was based on the assumption that the total energy equals the kinetic energy plus the fragment excitation energy, and that the latter follows a Poisson probability distribution. Although these are approximations, particularly since the pre-neutron-emission masses are not unique (the charge split *is* unique), the curves are a reasonable fit to the data and yield the average total kinetic energy. It is interesting to compare the average kinetic energy derived for a particular final isotope with that for all fissions yielding a fragment of the same mass. In Fig. 18 the points are based on events associated with a given γ ray, while the line is based on the two-parameter (fission-fragment-fission-fragment) calibration runs which are in good agreement with the measurements reported by Schmitt, Neiler, and Walter.[30] The points tend to lie slightly above the curve, on the average less than 2 MeV. Thus fissions producing the delayed γ rays exhibit slightly higher kinetic energy than the average for all fissions. Only the strongest γ rays were selected for this study, and hence the isotope selected probably lies near the peak of the
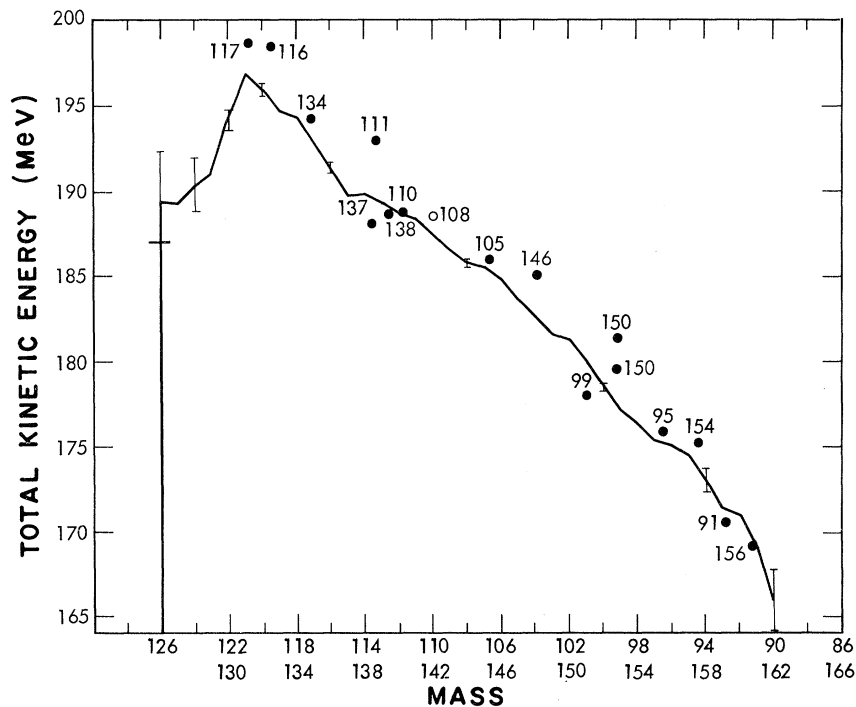
FIG. 18. Kinetic energy of fission versus preneutron mass split. The solid line is the result of two-parameter (fragment-fragment) runs. The plotted points are the average kinetic energies of fissions producing fragments that emit selected γ rays; these points are plotted at the preneutron mass and labeled with the postneutron mass.

charge distribution. One interpretation of the results is that such fissions produce greater kinetic energy.

V. CONCLUSIONS

In the present work detailed data have been obtained on the γ rays emitted from isomeric states of ^{252}Cf fission fragments in the time range of 3 to 2000 nsec after fission. The energies, intensities, and half-lives of 144 γ rays were determined, corresponding to between 80 and 100 isomeric states. Approximately 50% of the fragment isotopes have isomeric states. On the other hand, the intensity is concentrated into roughly four mass regions: 96, 108, 134, and 146.

The γ-ray energy spectrum consists of a group of transitions below ~500 keV and a group near 1300 keV, the latter emitted by fragments with masses near 134. A strong cascade from a 162-nsec isomeric state is assigned to ^{134}Te, and a 3000-nsec cascade to ^{136}Xe. The unusually high energy of the γ rays from these nuclei is explained by the fact that they have neutron number 82 and proton numbers near 50. While deformed nuclei are expected in some of the other mass regions with strong γ-ray yields, rotational cascades are not observed, in contradiction to the interpretations placed on earlier low-resolution work.

The energies and half-lives spanned by the data imply that the transitions are $E1$, $M1$, or $E2$, either allowed or K forbidden by a few units. Isomerism in fission fragments is thus similar to that occurring in nuclei near the line of stability. We conclude that the initially high spins of the fragments are less important in determining the character of the delayed γ rays than previously thought.

Comparison of the present data on delayed γ rays with data from other experiments on the γ rays, x rays, and conversion electrons from fission gives the atomic number of the isotope in a number of cases. Future work should result in additional identifications of the isomers observed here and expand the spectroscopic information on these neutron-rich nuclei.

Finally, fragment kinetic energy distributions were obtained for fissions leading to the emission of a particular γ ray, that γ ray serving to restrict the events to those having a definite final isotope for one fragment. The average kinetic energy of such events is found to be slightly higher than the average for all fissions leading to that mass.

VI. ACKNOWLEDGMENTS

*Work performed under the auspices of the U. S. Atomic Energy Commision.

†Major, U. S. Air Force; portions of the present work are based on a thesis submitted by F. Guy to the Graduate Division of the University of California, Davis, in partial satisfaction of the requirements for the Ph.D. degree in Engineering–Applied Science.

[1]S. A. E. Johansson, Nucl. Phys. 60, 378 (1964).

[2]S. A. E. Johansson and P. Kleinheinz, in *Alpha-, Beta-, and Gamma-Ray Spectroscopy*, edited by K. Siegbahn (North-Holland Publishing Company, Amsterdam, The Netherlands, 1965), Vol. 1, p. 805.

[3]The half-lives of the "delayed" γ rays which are discussed in the present paper are always much shorter than any possible β-decay half-lives.

[4]F. C. Maienschein, R. W. Peelle, W. Zobel, and T. A. Love, in *Proceedings of the Second United Nations International Conference on the Uses of Atomic Energy, Geneva, 1959* (United Nations, Geneva, Switzerland, 1958), Vol. 15, p. 366.

[5]S. A. E. Johansson, Nucl. Phys. 64, 147 (1965).

[6]L. A. Popeko, G. V. Valskii, D. M. Kaminker, and G. A. Petrov, J. Nucl. Energy Pts. A and B, 20, 811 (1966).

[7]R. B. Walton and R. E. Sund, Phys. Rev. 178, 1894 (1969).

[8]R. E. Sund and R. B. Walton, Phys. Rev. 146, 824 (1966).

[9]R. B. Walton, R. E. Sund, E. Haddad, J. C. Young, and C. W. Cook, Phys. Rev. 134, B824 (1964).

[10]The term "isomeric" is used throughout this paper to designate a transition with a measurable half-life, whatever that half-life might be.

[11]D. H. White, private communication.

[12]C. Chasman, K. W. Jones, and R. A. Ristinen, Nucl. Instr. Methods 37, 1 (1965).

[13]Rand L. Watson, University of California Radiation Laboratory Report No. UCRL-16798 (unpublished).

[14]H. R. Bowman, J. C. D. Milton, S. G. Thompson, and W. Swiatecki, Phys. Rev. 126, 2120 (1962); 129, 2133 (1963).

[15]H. W. Schmitt, W. E. Kiker, and C. W. Williams, Phys. Rev. 137, B837 (1965).

[16]W. E. Nervik, Phys. Rev. 119, 1685 (1960).

[17]J. Kantele and O. Tannila, Nucl. Data A4, 359 (1968).

[18]W. John, J. J. Wesolowski, and F. Guy, Phys. Letters 30B, 340 (1969).

[19]H. Albinsson and L. Lindow, private communication.

[20]C. F. Perdrisat, Rev. Mod. Phys. 38, 41 (1966).

[21]M. Goldhaber and A. W. Sunyar, in *Alpha-, Beta-, and Gamma-Ray Spectroscopy*, edited by K. Siegbahn (North-Holland Publishing Company, Amsterdam, The Netherlands, 1965), Vol. 2, Chap. 18.

[22]L. S. Kisslinger and R. A. Sorensen, Kgl. Danske Videnskab. Selskab, Mat.-Fys. Medd. 32, No. 9 (1960).

[23]J. P. Unik, private communication.

[24]A. Lundan and A. Siivola, Ann. Acad. Sci. Fennicae A6, No. 288 (1968).

[25]N. R. Johnson and G. D. O'Kelley, Phys. Rev. 114, 279 (1959).

[26]P. A. Moore, P. J. Riley, C. M. Jones, M. D. Mancusi,

and J. L. Foster, Jr., Phys. Rev. C 1, 1100 (1970).

[27]R. L. Watson, J. B. Wilhelmy, R. C. Jared, C. Rugge, H. R. Bowman, S. G. Thompson, and J. O. Rasmussen, Nucl. Phys. A141, 449 (1970).

[28]J. B. Wilhelmy, University of California Lawrence Radiation Laboratory Report No. UCRL-18979, 1969 (unpublished).

[29]T. Alvager, R. A. Naumann, R. F. Petry, G. Sidenius, and T. Darrah Thomas, Phys. Rev. 167, 1105 (1968).

[30]H. W. Schmitt, J. H. Neiler, and F. J. Walter, Phys. Rev. 141, 1146 (1966).

Measurements of Static Quadrupole Moment of the First Excited 2^+ States of the Nuclei Pd^{106} and Pd^{110} by Heavy-Ion Coulomb Excitation*

R. Beyer,[†] R. P. Scharenberg, and J. Thomson

Department of Physics, Purdue University, Lafayette, Indiana 47907

(Received 27 April 1970)

The static quadrupole moments of the 511.7-keV 2^+ state in Pd^{106} and the 373.8-keV 2^+ state in Pd^{110} have been determined by employing Coulomb-excitation techniques. Foils (~175 $\mu g/cm^2$) of separated Pd isotopes were bombarded with 25- and 30-MeV O^{16} ions and 55- and 56-MeV S^{32} ions from the Purdue University and Argonne National Laboratory tandem accelerators. The angular distributions of the inelastically scattered ions were measured in coincidence with the deexcitation γ rays to determine the relative excitation probabilities. The experimental data were fitted using the Winther–de Boer multipole-Coulomb-excitation program so that the sign and magnitude of the static quadrupole moment could be extracted. The effect of higher excited states on the excitation probability of the 2^+ state has been calculated using the matrix elements determined by Robinson *et al.* and the Winther–de Boer program. Self-consistency of the oxygen and sulfur data suggests that the excitation via the second 2^+ state interferes constructively so as to increase the excitation probability. With this choice for the interference via the second 2^+ state, the values of the static quadrupole moments are $Q_{22} = -0.458 \pm 0.059$ b for Pd^{106} and $Q_{22} = -0.483 \pm 0.049$ b for Pd^{110}. If the excitation via the second 2^+ state interferes destructively, the values of the static quadrupole moments are $Q_{22} = -0.282 \pm 0.059$ b for Pd^{106} and $Q_{22} = -0.266 \pm 0.049$ b for Pd^{110}.

I. INTRODUCTION

The Pd isotopes are classic examples of vibrational nuclei. In Pd^{106} and Pd^{110}, both the one-phonon 2^+ state and the two-phonon 0^+, 2^+, 4^+ triplet states are present, as predicted by the pure vibrational model of the nucleus.[1,2] The Pd nuclei, therefore, can be considered good subjects on which to test predictions of the vibrational model of the nucleus. One prediction of this model is that the static electric quadrupole moment of the first quadrupole phonon (2^+) state should be zero. Recent experiments[3-10] have shown substantial static quadrupole moments for these states in vibrational nuclei.

Tamura and Udagawa[11] are able to account for substantial static quadrupole moments by con-

sidering the first and second excited 2^+ states to be composed of large admixtures of the one- and two-quadrupole phonon states in their anharmonic-vibrator model of the nucleus. The results of this experiment will be compared with the predictions of the anharmonic-vibrator and the pure rotational models of the nucleus.

The reorientation effect[12] can be the dominant interference effect in heavy-ion Coulomb excitation. The reorientation effect involves the interaction of the static electric quadrupole moment of the target nucleus in its excited state and the electric field gradient produced by the incident projectile. Since this electric field gradient can be computed, the value of the static quadrupole moment of the nucleus can be extracted by measuring the relative differential excitation cross